Comparison of Soil-Structure Interaction Effects between Building Code Requirements and Shake Table Study

N. Hosseinzadeh[1], M. Davoodi[2], and E. Rayat Roknabadi[3]

1. Assistant Prof., Structural Engineering Research Center, International Institute of Earthquake Engineering and Seismology (IIEES), Tehran, I.R.Iran, email: hosseinz@iiees.ac.ir;
2. Assistant Prof., Geotechnical Engineering Research Center, International Institute of Earthquake Engineering and Seismology (IIEES), Tehran, I.R. Iran
3. MSc Student., International Institute of Earthquake Engineering and Seismology (IIEES), Tehran, I.R.,Iran

ABSTRACT

In this paper the dynamic soil-structure interaction effects on the seismic response of building structures with surface and embedded mat foundations have been studied using shake table tests on scaled models. Results obtained from test and analysis are compared with buildings code requirements. For this purpose, four structural models with 5, 10, 15 and 20 floors as common representative buildings in an urban area are designed and constructed for dynamic tests. Both soft and relatively soft soil media are considered in this study. Different parameters have been studied in this research which includes: building aspect ratio, shear wave velocity, frequency content, damping and acceleration of structural models. Also, the results of finite element analysis of soil-structure system compared with shake table results. The effects of soil-structure interaction is demonstrated as increasing the period of vibrations and damping ratio with a dominant rocking mode in higher buildings. However, these effects is reducing by increasing the embedment effects of foundation. Morever, the results of this research is important for developing of Soil-Structure-Interaction in national codes.

Keywords:
Soil-structure interaction;
Building structures;
Dynamic tests;
Shake table;
Embedded foundations

1. Introduction

With expansion of technology and urbanization, widespread and extensive projects are designed and implemented, some of which should be implemented at the adverse Geotechnical conditions. Over time, scale and size of these projects increases and in these circumstances, due to non considered conditions or unknown factors, confidence and character design and project cost increases. One of these factors, when dynamic load modified into structures is soil-structure interaction. Dynamic response analysis of structures under earthquake loads is one of the main tasks of earthquake engineering. Determining the stress and displacement of structures under dynamic loads such as earthquake is the most important issues in dynamic structure. But in general, structures are in action with the surrounding soil, and therefore incoming loads to the surrounding soil of the structure, should be considered during the earthquake stimulations. Compared with the structure, soil has an unlimited scope that wave propagation conditions should be considered in dynamic model. In recent years, many studies have been undertaken on dynamic soil-structure interaction for different types of structures, especially for heavy and massive structures, such as nuclear power plants, dams, coastal platforms, bridges and tall structures on the soft soil, among which the dynamic soil-structure interaction is very important [1].

There are limited criteria in building code requirements for investigation of soil-structure interaction effects, for example, the *NEHRP* provisions code which investigate the soil-structure interaction effects on seismic structural plan can be pointed out, but these rules did not provide any specific criteria for buried foundation. Unfortunately, Iran's codes and criteria such as 2800 Iran earthquake code, does not offer specific rules in this regard. Therefore a comparison of soil-structure interaction effects between building code requirements and shake table study is important for completion of building code requirements. Complete information from back-grounds and different methods of soil-structure interaction analysis has been cited on the references [2-4].

Dynamic soil structure interaction occurs during the passage of earthquake waves through the soil structure system. It involves scattering of the incident waves from the foundation system, transfer of incident wave energy into the structure, and radiation of the structural vibration energy back into the soil. During this process, the motion of the soil is altered relatively to what it would have been in the absence of the structure. Also, the motion of the building is different from what it would have been if the soil were rigid. Because of soil-structure interaction, the soil experiences additional motion.

In a more general sense, the soil-structure interaction is a collection of phenomena in the response of structures caused by the flexibility of the foundation soils, as well as in the response of soils caused by the presence of structures. Modeling of its effects requires additional degrees-of-freedom, and for some applications use of wave propagation methods. In general, it lengthens the apparent system period, increases the relative contribution of the rocking component of ground motion to the total response, and usually reduces the maximum base shear. The reduction of structural response results from the scattering of the incident waves from the foundation, and from radiation of the structural vibration energy into the soil. When the soil surrounding the foundation experiences small to moderate levels of nonlinear response, the soil structure interaction lead to significant absorption of the incident wave energy, thus reducing the available energy to excite the structure. An important challenge for future seismic design is to quantify this loss and exploit it in design of soil-structure systems [2].

In the present study, the authors have attempted to evaluate the seismic response characteristics of surface and embedded model buildings using experimental tests on the shaking table. Shaking table tests and finite element analysis of four steel building models with 5, 10, 15, and 20 stories have been studied in this paper for accounting the soil-structure interaction effects in the case of surface and embedded buildings. Successful results of shaking table model tests show the feasibility of 1-g scale modeling technique. Also, a good agreement has been shown between shaking table test results and finite element analysis.

2. Finite Element Method

The finite element formulation in dynamic soil and foundation problems implies a step further in the approximations for the definition of the soil media. It requires a discretization and a finite element definition of a determinate soil volume. This discretization alone would trap the energy of the system and distort its dynamic characteristics. To avoid this problem, the finite element formulation is often coupled with a transmitting boundary formulation. The resulting formulation is usually referred as Dynamic Finite Element Method. The transmitting boundary simulates the wave propagation into the exterior semi-infinite media and expresses the far-field in terms of a free-field behavior (isolated from the interaction with any other mechanical system). In the original formulation, the transmitting boundary was coupled with a discrete volume which included the foundation as well as the surrounding soil affected by the interaction with the structure. Therefore, it was set relatively far away from the foundation. Further improvements were reached with the Flexible Volume Method. This included the definition of the whole layered media in the mathematical formulation, avoiding the requirement to set the transmitting boundary relative far away from the foundation. The transmitting boundary was then attached to a simpler discretization: a vertical column of quadrilateral elements for 2-*D* configurations and a vertical column of cylindrical elements for 3-*D* configurations. The mechanical formulation of this discrete region was expressed in terms of finite element approximations. This formulation was repeated on every common soil-foundation node to compute the stiffness matrix of the whole layered media [5].

3. Inertial and Kinematic Interaction

Two physical phenomena that comprise the soil-structure interaction mechanisms are inertial interaction and kinematic interaction. The inertial interaction due to structural vibrations gives rise to the horizontal and rocking motion of the foundation relative to the free-field. Frequency dependant of foundation impedance functions describes the flexibility of the foundation support as well as the damping associated with foundation soil interaction.

The kinematic interaction is the deviation of stiff foundation motions as a result of ground motion incoherence, wave inclination, or foundation embedment. These effects are described by a frequency dependent transfer function relating the free-field motion to the motion that would occur on the base slab if the slab and structure were massless. Kinematic interaction indicates the effects of rigid massless foundation slab- the so-called "τ factor". This factor is defined as the ratio of the amplitudes of the harmonics in the rigid-base translational motion to the corresponding free-field amplitudes.

A system commonly employed in simple field analysis of inertial interaction is shown in Figure (1), which consists of a single-degree-of-freedom structure of height *h*, mass *m* stiffness *k* and damping *c* on a flexible foundation medium. The base flexibility including translation (u_f) and rotation (θ) is represented by complex stiffness $\overline{K}_y$ and $\overline{K}_\theta$. The real static stiffness K_u and K_θ of a rigid disk on a half space is defined by:

$$K_u = 32\frac{1-\mu}{7-8\mu}Gr_\circ \quad (1)$$

$$K_\theta = 8\frac{1}{3(1-\mu)}Gr_\circ^3 \quad (2)$$

Where *G* is the soil dynamic shear modulus, μ is the soil Poisson ratio, and $r_\circ$ is the foundation radii corresponding translation and rotation deformation modes to match the area and moment of inertia of the actual foundation.

The flexible base parameters including effective period $\tilde{T}$ and effective damping $\tilde{\beta}$ are evaluated as follows:

$$\tilde{T} = T\sqrt{1+\frac{\overline{K}}{K_u}\left(1+\frac{K_u\overline{h}^2}{K_\theta}\right)} \quad (3)$$

$$\tilde{\beta} = \beta_\circ + \frac{0.05}{\left(\frac{\tilde{T}}{T}\right)^3} \quad (4)$$

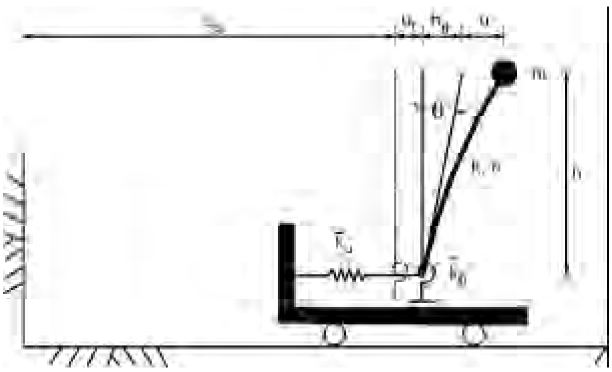

Figure 1. Experimental model of soil-structure interaction system [6].

Where $T = k/m$ is the fixed base period, and $\beta_\circ$ is foundation damping factor. Simplified soil-structure interaction provisions are included in *NEHRP*-2003 codes based on the above equations [7].

4. Experimental Approach

Dimensional analysis are the framework for the scale model similitude in this test program. Three principle test conditions established for scaling parameters are as follows:

1. Testing is conducted in a 1-*g* environment, which defines model and prototype accelerations to be equal.
2. A soil model with similar density to the prototype soil is desired, which fixes another component of the scaling relations
3. The test medium is primarily composed of saturated clay, which undrained stress-strain response is independent of confined pressure, thereby simplifying the constitutive scaling requirements.

Four structural models of 5, 10, 15 and 20 stories high and two relatively soft soil models were designed for the laboratory tests. The foundation system of structural models was considered as square rigid mats. In all building models, the height of each storey is 3*cm* and the dimension of square rigid surface mats is 20_20*cm*. A geometrical scaling of 1/100 is considered for both soil and structure models [4]. A special cylindrical flexible-wall container was designed and constructed to support the soil model with special emphasis on easy connection to the shake table. This container also provided sufficient environment to allow for the elastic half space of the soil. The diameter of ground specimen is 120*cm* and the thickness of homogeneous single soil layer from the base rock is 60*cm*. General view of structural models, single soil-structure interaction models and very low mass accelerometers for vibration recordings are shown in Figures (2) to (4) respectively [4].

Horizontal component of scaled motions of El Centro 1940 (*USA*) and Tabas 1981 (*I.R.*) earthquakes with different Peak Ground Accelerations (*PGA*) was used as the inputs for the shaking table. Experimental tests have been carried out in the International Institute of Earthquake Engineering and Seismology (*IIEES*) one-component shaking table in I.R. Iran [4]. The dimension of this table is 120x140*cm* and the capacity of hydraulic jack is 50*KN*.

The complete shaking table test program including four steps is summarized as follows. These steps are repeated in two phases for two soil types *III* and *II* as defined in Iran seismic code (standard 2800) [8].

1. Fixed base structural models.
2. Free-field response of soil models.
3. Soil-structure interaction tests for the surface structure models.
4. Soil-structure interaction test for the embedded structure models.

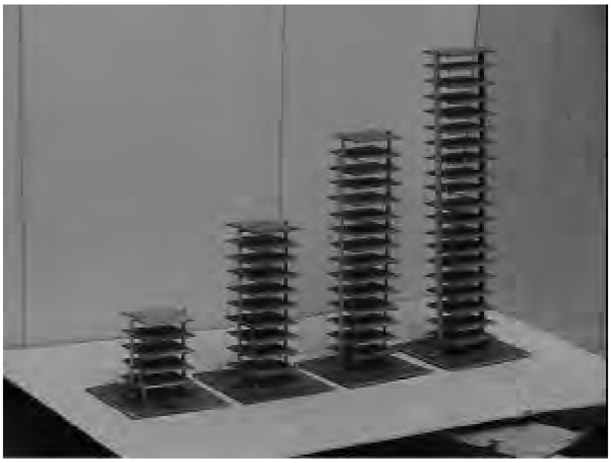

Figure 2. Structural Models.

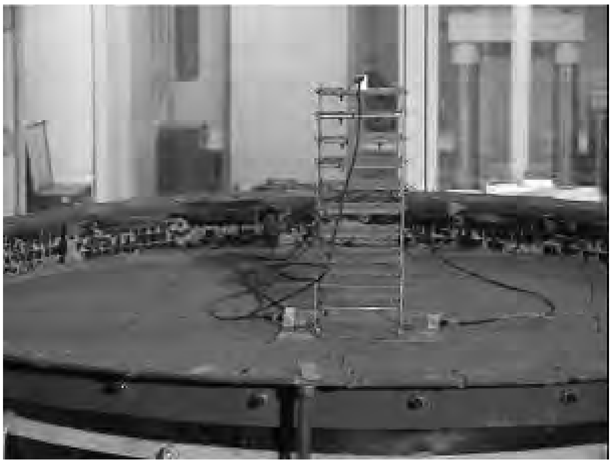

Figure 3. Single Structure on the soil.

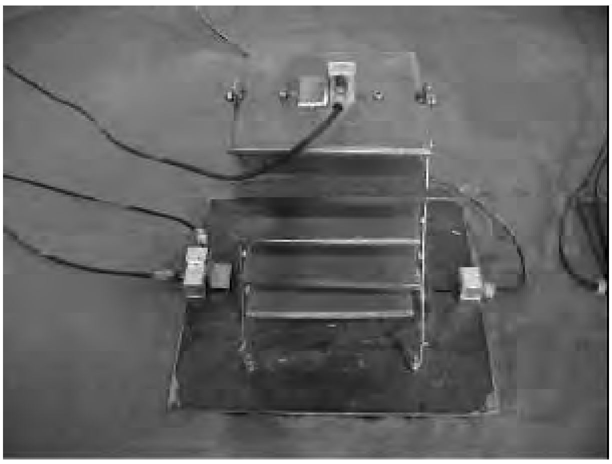

Figure 4. Measuring accelerometers on the structure and foundation.

Before the main tests program, some preliminary tests were considered to evaluate the performance of the shaking table . A typical test series for an individual model were consisted of a hammer blow test, a sine sweep test, the El Centro motion, the Tabas motion, another sine sweep test, and a final hammer blow test.

5. Test Results

A comparison between command signals and the shaking table shows that the table response match to the command signal and is good and repeatable. Therefore, the results obtained from several model tests are comparable. Some important free-field response test results are as follows. These results are presented in the real scale.

Based on the soil dynamic laboratory tests and shaking table tests, the soil properties were determined at small amplitude strains. In accordance to *ASTM* standard, the soil type was classified as Silty clay (*CL-ML*). The results of shear wave velocity (V_s), resonant frequency (f_n), and damping ratio (D) in small excitations are summarized in Table (1). This frequency is very close to that obtained from the analytical equation determined for a homogeneous soil layer of thickness H_s underlain by a rock or rocklike material [9].

$$\omega_n = \frac{(2n-1)\pi}{2H_s} V_s \tag{5}$$

Where n is the nth mode and V_s is the shear wave velocity that can be determined from shear modulus (G) and density of soil (ρ) as follows:

$$V_s = \sqrt{\frac{G}{\rho}} \tag{6}$$

6. Numerical Method

Due to the complexity of full scale finite element models it is helpful to perform preliminary tests on

Table 1. Frequency content and damping ratio of soil model in small excitations.

Soil Type	V_s (*m/s*)	Test Frequency (f_n) (*Hz*)	Anal Frequency (Eq. (5)) (*Hz*)	Damping (%)
III	310	1.3	1.33	4.2
II	430	1.8	1.79	4.1

simplified models in order to verify the adequacy of the time and mesh discretization with respect to the input motion. It also provides good insight in the performance of the nonlinear material model. Therefore, a series of tests on a one-dimensional soil column have been proposed as follows:

- Static pushover test on nonlinear soil column to obtain the nonlinear behavior of the material model.
- Dynamic test of elastic soil column by applying an earthquake motion to the elastic soil column. Using this test it can be investigated that whether the selected grid spacing is capable of representing the motion correctly without filtering out any relevant frequencies. This test also allows choosing appropriate damping parameters. It should be noted that this is additional (small) damping that is used for stability of the numerical scheme and should not be relied upon to provide major energy dissipation. It seems that major energy dissipation should result from inelastic deformations of the *SFS* system.
- Dynamic test of nonlinear soil column for investigation of the stability and the accuracy of the numerical method can be examined by applying the earthquake motion to the nonlinear column of soil. A second analysis with a time step reduced by 50% may tend to a significantly different result. Furthermore it will be examined how propagation through an elastic-plastic material will change the frequency content of the motion [10].

6.1. Model Description

The material properties of the soil are given in Table (2). The discretization parameters, the maximum grid spacing *Dh* and the time step *Dt* are determined as follows:

$$Dh \le \frac{V_s}{10 f_{max}} = \frac{310}{10 \times 10} = 3.1m \tag{7}$$

For the following analysis $Dh = 3m$ is selected. Therefore, the maximum time step is:

$$Dt \le \frac{D_h}{V_s} = \frac{3}{310} = 0.0096s \tag{8}$$

Table 2. The material properties of the soil.

Friction angle (f)	41.2°
Undrained shear strength (C_u)	10 KPa
Mass density (?)	1900 Kg/m^3
Shear wave velocity (V_s)	310m/s

Taking into account a further reduction of the time step, about 60% for nonlinear material models $Dt = 0.0055s$ is chosen.

6.2. Static Pushover Test on Elastic-Plastic Soil Column

For the static pushover test, an elastic perfectly plastic Von-Mises material model is used. After applying self weight a horizontal load of 3.4*KN* is applied to a surface node. The predicted shear strength of the first element that is expected to fail, the one at the surface, is:

$$\begin{aligned}\tau_f &= C_u + z \times \rho \times g \times tan(\varphi) = \\ &10 + 0.5 \times 1.9 \times 9.81 \times tan(41.2^\circ) = 18.16KPa\end{aligned} \tag{9}$$

Where z is the depth of the center of the first element, τ_f is shear strength, C_u is undrained shear strength, ρ is Mass density and φ is friction angle.

Figure (5) shows the shear stress versus shear strain of soil for the first element obtained from pushover analysis. The maximum stress obtained is 18.61*KPa* that is 2.5% which differs from the theoretical value. The initial slop in diagram (linear mode) obtained from the soil shear modulus, $G = 182585KPa$, has little difference from the value obtained from test results ($G = 182590KPa$). Therefore, the soil behavior in the finite element model is almost similar to the existing theoretical values.

6.3. Dynamic Test on Elastic Soil Column

In order to test the spatial discretization of the model, an earthquake motion is propagated through an elastic soil column. The grid spacing of the finite element mesh can be selected so that the upper frequencies (up to $f_{max} = 10Hz$) are represented accurately in the numerical analysis. Calculation of the transfer functions between the base and the surface of the soil column is a good way in this regard. Transfer functions do not depend on the input motion; therefore

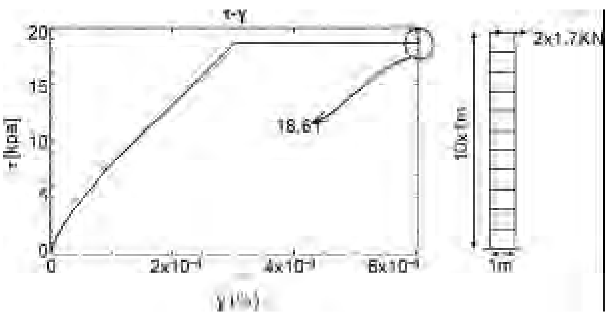

Figure 5. Shear stress-strain obtained from pushover analysis.

it can be easily compared with closed form solutions.

The transfer function of a soil deposit describes the amplification between the frequencies of the motion at the base and at the soil surface and can be determined from the following [10]:

$$TF(\omega) = \frac{1}{\cos(\omega H \sqrt{\frac{\rho}{G + i\omega\zeta}})} \tag{10}$$

Where H is the thickness of the soil deposit above the bedrock, ω is the circular frequency, and ζ is the damping coefficient.

Figure (6) shows a comparison between the closed form solution and the numerical transfer functions obtained from the finite element analysis. Rayleigh damping is used to obtain the damping matrix C:

$$C = \alpha M + \beta K \tag{11}$$

The analysis is performed using stiffness proportional Rayleigh damping of $\beta = 0.001$ and $\beta = 0.01$ and no mass proportional damping is applied ($\alpha = 0$). It can be seen that the numerical transfer functions are very close to the closed form solution. Based on the above observations a stiffness proportional Rayleigh damping of $\beta = 0.01$ is selected for the finite element analysis. This value of damping eliminates the effects of frequencies above $10Hz$ appropriately.

6.4. Dynamic Test on Elastic-Plastic Soil Column

In the next step, Von-Mises elastic-plastic material model has been selected. The analysis was performed using time steps of $dt = 0.0055s$ and $dt = 0.0028s$. Figure (7) shows the output acceleration and response spectra of free-field surface. As shown in this Figure, there is an acceptable agreement between the two analysis. Therefore, the analysis is performed using $dt = 0.0055s$.

7. Soil Modulus Curve

Variation of shear modulus with shear strain is the most important parameter for the free-field surface response analysis. Shear modulus versus shear strain curve (G-γ curve) can be obtained using the tri-axial test as shown in Figure (8). In this figure Seed and Idriss [11] proposed a curve for the undrained clay. The other curve shown in this figure is known as calibration curve, which is obtained from comparison of free-field response of finite element results with the shake table results. This means that the soil shear modulus is considered so that the analytical results are compatible with the experimental results for earthquake excitations with different intensities.

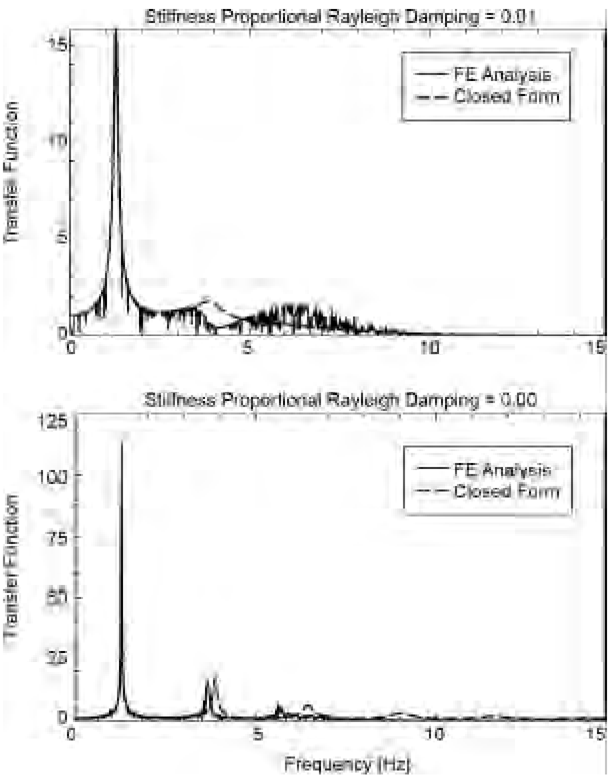

Figure 6. Transfer function of finite element and closed form solutions.

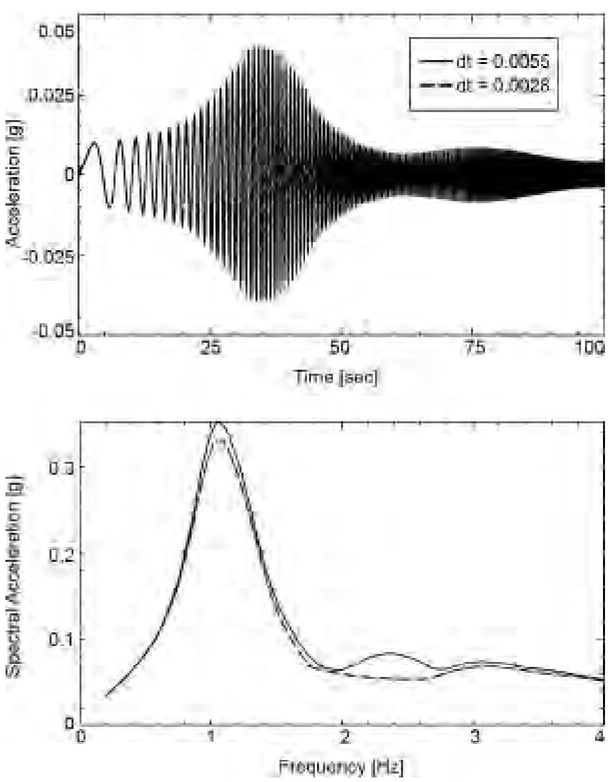

Figure 7. Acceleration responses for free-field analysis with dt = 0:0055 and dt = 0:0028s.

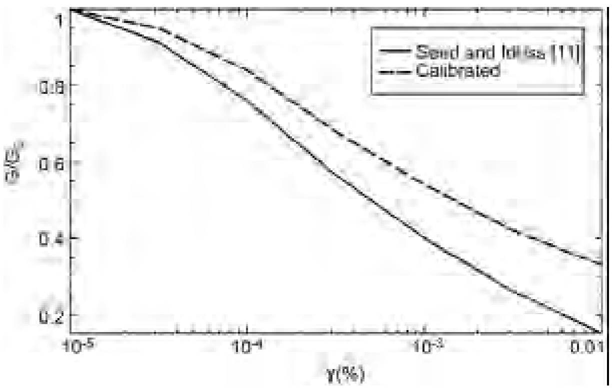

Figure 8. Shear modulus-shear strain curve.

8. Comparison between Analysis and Test Results

For analytical models OpenSees software is used. Investigations indicate a very good agreement between analysis and experimental results of the free-field and structural models top responses. For example, Figure (9) shows a comparison between acceleration output from the analysis and testing soil model. Most differences are related to the response of higher modes of vibration. Minor differences in experimental and analysis results are related to the laboratory errors and numerical modeling assumptions.

9. Frequency and Damping of Structural Model

A review between test and analysis results of structural models in high amplitude input motions (*PGA* 0.3*g*) is shown in Tables (3) and (4). The results of these tables show the important effects of *SSI* in reducing the frequencies and increasing the damping ratios of structural models in comparison to fixed base models. The frequencies obtained from the analysis

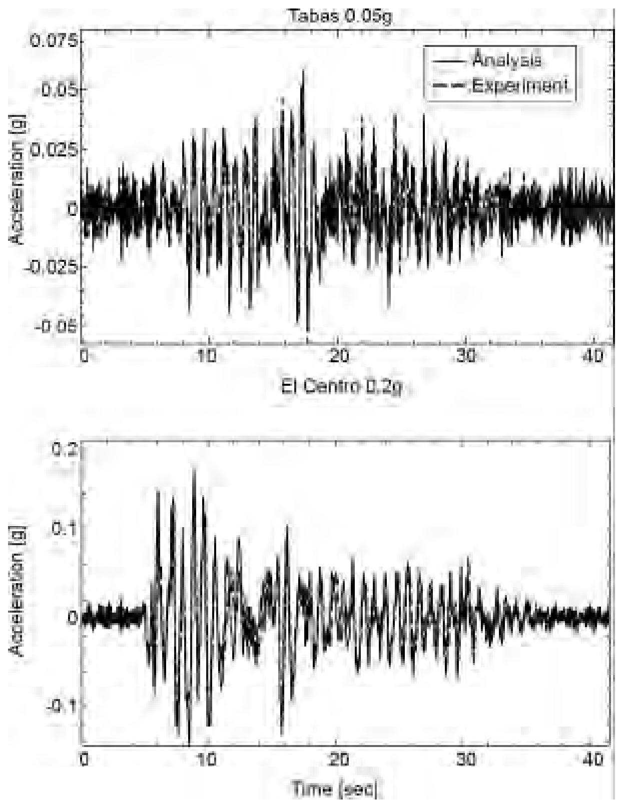

Figure 9. Comparison of analytical and experimental results.

and tests are in good agreement, except in the case of 10 story model. The beam-column connections of experimental model of this structure was performed as semi-rigid connections. Therefore, the high damping observed in this test model is related to the special behavior of its connections.

10. Investigation of Code Requirements

In this section, a comparison between test and analysis results of this study has been made with

Table 3. Comparison between experimental and analysis frequencies (Hz).

Structural Model	Fixed		With SSI (Surface)		With SSI (Embedded)	
	Experiment	Analysis	Experiment	Analysis	Experiment	Analysis
5 story	1.55	1.55	1.54	1.54	-	1.54
10 story	0.8	0.82	0.68	0.792	-	0.799
15 story	0.54	0.533	0.50	0.51	0.518	0.518
20 story	0.374	0.377	0.355	0.355	0.363	0.363

Table 4. Comparison between experimental and analysis damping ratio (%).

Structural Model	Fixed		With SSI (Surface)		With SSI (Embedded)	
	Experiment	Analysis	Experiment	Analysis	Experiment	Analysis
5 story	0.43	0.66	0.93	1.18	-	1.12
10 story	7.03	6	2.9	13	-	12.5
15 story	1.45	1.98	2.26	2.7	1.47	2.77
20 story	1.57	1.82	2.58	2.47	2.42	2.35

NEHRP and *ATC* code requirements. Important soil-structure interaction effects in these codes are summarized in the effective period and the effective damping ratio of the dominant first mode of vibration.

10.1. Comparison of the Effective Period

The effective period $(\tilde{T})$ based on the *NEHRP* requirements is determined from Eq. (3). In this equation K_u and K_θ are horizontal and rocking stiffnesses, respectively. A large value of K_u means that only rocking mode is participated in *SSI* effects. Variation of effective period versus the ratio of $\bar{h}/r$ is shown in Figure (10) to Figure (12) for soil types *III* and *IV*. As shown in these figures, the effect of horizontal and rocking mode has similar effects on the low values of this ratio. However, by increasing the $\bar{h}/r$ ratios, the rocking mode will be dominant. Comparison of these results with *NEHRP* recommendations indicates good agreement and similar trends. However, *NEHRP* recommendation is in lower bound for determination of effective periods especially in the higher range of $\bar{h}/r$ ratios.

10.2. Comparison of the Effective Damping

The effective damping ratio $(\tilde{\beta})$ based on the *NEHRP* requirements is determined from Eq. (4). In this equation β is the fixed base period and damping ratio, and $\beta_\circ$ is the foundation damping factor. Variation of effective damping ratios versus the ratio of $\bar{h}/r$ is shown in Figure (13) for soil types *III*. As shown in this figure, by increasing the $\bar{h}/r$ ratios, the effective damping ratio decreases. Comparison of these results with *NEHRP* recommendations indicates good agreement. However, *NEHRP* recommendation is in upper bound for determination of effective damping especially in the higher range of $\bar{h}/r$ ratios.

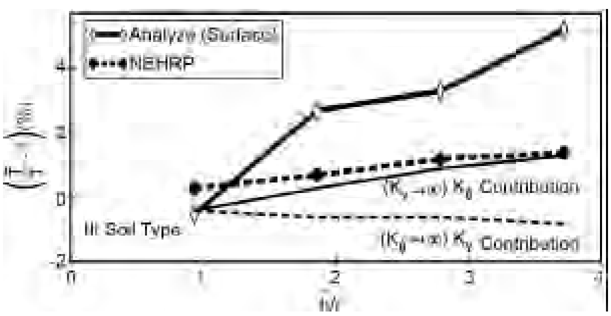

Figure 10. Variation of fundamental period of structural models with $\bar{h}/r$ ratios in surface foundations (soil type III).

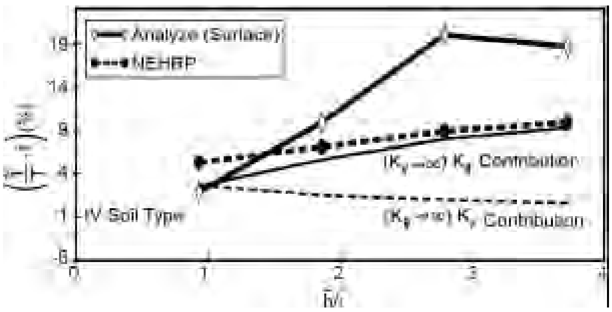

Figure 11. Variation of fundamental period of structural models with $\bar{h}/r$ ratios in surface foundations (soil type IV).

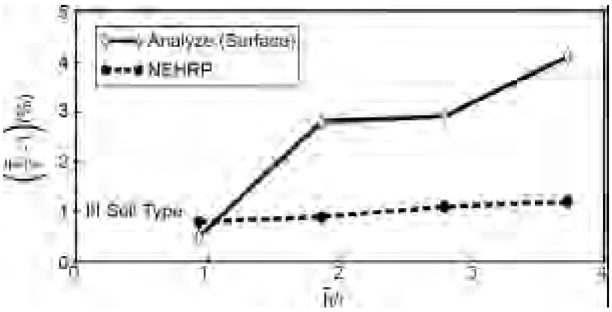

Figure 12. Variation of fundamental period of structural models with $\bar{h}/r$ ratios in embedded foundations (6m embedded structure or about 2 story embedment).

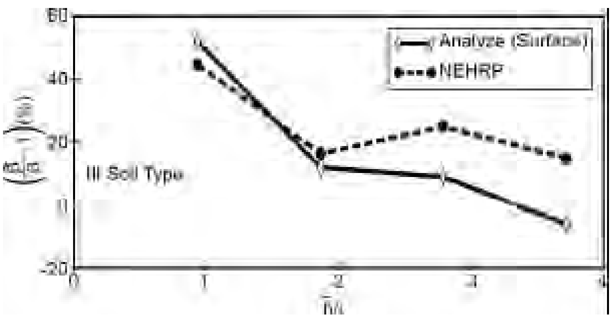

Figure 13. Variations of structural damping with $\bar{h}/r$ (soil type III).

11. Conclusions

In this paper, four structural models 5, 10, 15 and 20 floors as common representative of real buildings in urban area (such as Tehran) are designed and constructed for experimental study of *SSI* (Soil-Structure Interaction) effects on the shake table. Two soil type *III* (V_s = 310*m/sec*) and *II* (V_s = 430*m/sec*) have been considered in this study based on the standard *IR*2800. Also, an additional soil type *IV* (V_s = 150*m/sec*) has been selected for the analytical study. With regard to the experimental-analytical study performed in this paper, the following conclusions have been obtained:

- A good agreement between experimental and finite element numerical modeling results has been observed. This agreement is very good especially for free-field responses. Generally good agreement between experimental-analytical responses has been observed in fundamental mode response of soil and structure system, but some differences can be seen in higher mode responses of structural models. These differences are related to laboratory test errors and analytical simulations.
- A comparison of Experimental-Analytical model results with *NEHRP* recommendations indicates that by increasing the building aspect ratio ($\bar{h}/r$), the effective period of the building increases, but the variation rate of experimental- analytical models is higher than the code requirements.
- The *SSI* effects are dominant in fundamental mode of vibration both in the Experimental-Analytical study performed in this research and in the *NEHRP* provisions.
- The horizontal and rocking modes of foundation are the main mechanism of *SSI* effects. In lower story buildings with aspect ratio of $\bar{h}/r = 0.93$, the contributions of these modes are almost equal. However, in higher buildings with ratio of $\bar{h}/r > 2.8$, the rocking mode of foundation is dominant.
- The fundamental period of *SSI* models in embedded foundations is lower than in the surface foundations. This means that in the case of embedded foundation, the effects of *SSI* are lower than the surface foundations.
- The damping ratio in the case of embedded foundations is lower than the surface foundations. However, the embedment effects in low rise buildings are negligible.

References

1. Gatmiri, B. and Haeri, S.M. (1996). "Guidelines of SSI Analysis and its Effects on Dynamic Response of Structures", *Natural Disaster Defense Research Center*, First Edition (in Farsi).

2. Trifunac, M.D., Hao, T.-Y., and Todorovska, M.I. (2001). "Full-Scale Experimental Studies of Soil-Structure Interaction", *2nd U.S.-Japan Workshop on Soil-Structure Interaction*, Tsukuba City, Japan, March 2001.

3. Bazyar, M.H. and Khani, M. (2007). "Dynamic Soil-Structure Interaction Analysis Using the Scaled Boundary Finite Element Method", PhD thesis, School of Civil and Environmental Engineering, The University of New South Wales, Sydney, Australia.

4. Hosseinzadeh, N.A. (2002). "Shake Table Study of Soil-Structure Interaction Effects on Seismic Response of Single and Adjacent Buildings", PhD Thesis, IIEES, Tehran, Iran.

5. Julio Abraham Garcia, M.I. (2002). "Reduction of Seismically Induced Structural Vibrations Considering Soil-structure Interaction", PhD thesis, Bochum.

6. Stewart, J.P., Seed, R.B., and Fenves, G.L. (1998). "Empirical Evaluation of Inertial Soil-Structure Interaction Effects", Technical Report PEER-98/07, Pacific Earthquake Engineering Research Center, University of California, Berkeley, California.

7. Building Seismic Safety Council (1997). "NEHRP Recommended Provisions for Seismic Regulations for Near Buildings", Rep. No. FEMA 222 A.

8. Iranian Code of Practice for Seismic Resistant Design of Buildings (Standard 2800) (1998). BHRC, Second Edition.

9. Das, B.M. (1993). "Principles of Soil Dynamics", PWS-KENT Pub.

10. Jeremic, B., Yang, Zh., Cheng, Zh., Jie, G., Sett, K., Taiebat, M., Preisig, M., and Tafazzoli, N. (2008). "Lecture Notes on Computational Geomechanics: Inelastic Finite Elements for Pressure Sensitive Materials, Chapter 8", Technical Report, Dept. of Civil and Environmental Engineering, University of California, Davis, USA.

11. Seed, H.B. and Idriss, I.M. (1969), "Influence of Soil Conditions on Ground Motions During Earthquakes", *Journal of Soil Mech. and Found. Div., ASCE*, 9(SM1), 99-137.